Fabrication of nonwoven polyester fabric supported grafted/crosslinked cellulose acetate reverse osmosis membrane for water desalination

Yasmeen Elkony[a,b,]*, Shaker Ebrahim[c], El-Sayed Mansour[a], Amel Elhusseiny[a], Eman Fadl[a], Hammed Hassan[a]

[a]*Chemistry Department, Faculty of Science, Central Lab at Ministry of Health, Alexandria University, P.O. Box: 426-Ibrahimia, 21321-Alexandria, Egypt, Tel. +20 1009980227; emails: igsr.yasmeen.elkony@alexu.edu.eg (Y. Elkony), ememansour@hotmail.com (E.-S. Mansour), amelelhusseiny@gmail.com (A. Elhusseiny), eman_fadl@yahoo.com (E. Fadl), hamed.hassan@alexu.edu.eg (H. Hassan)*
[b]*Central Laboratory at Ministry of Health, Alexandria, Egypt*
[c]*Department of Materials Science, Institute of Graduate Studies and Research, Alexandria University, Egypt,*
email: shaker.ebrahim@alexu.edu.eg (S. Ebrahim)

Received 3 December 2019; Accepted 6 June 2020

ABSTRACT

The main objective of this work is to prepare cellulose acetate (CA) reverse osmosis (RO) membranes supported onto nonwoven polyester fabric to withstand the applied high pressure. The supported CA-RO membrane with a 250 μm was selected to investigate the surface modification by grafting *n*-isopropyl acrylamide (N-IPAAm) and crosslinking with N,N'-methylenebisacrylamide (MBAAm). The surface roughness of the modified grafted and crosslinked membranes were measured with different areas of 0.5 μm × 0.5 μm, 1 μm × 1 μm and 5 μm × 5 μm by atomic force microscope. Average roughness (R_a) values were decreased from 5.51 to 1.27 nm and 2.31 nm for the unmodified CA-RO, the grafted and grafted/crosslinked supported-CA-RO membranes, respectively. The performance of the fabricated supported CA-RO membranes was tested and proved the high stability to 30 bar. It was found that the salt rejections of pristine supported CA, 0.1% N-IPAAm grafted supported CA and 0.1 N-IPAAm/0.013% MBAAm/supported CA-RO membranes were 85.91%, 92.4% and 96.4%, respectively. Moreover, it was noticed that the water flux values were 6 L/m²h for the unmodified supported membrane, 3.89 L/m²h for the grafted membrane and 3.75 L/m²h for the crosslinked/grafted supported CA-RO membrane at 14 bar.

Keywords: Cellulose acetate; Reverse osmosis; Membrane; Grafting; Crosslinking

1. Introduction

The most popular technology for water desalination is reverse osmosis (RO) membranes. The desalination process has provided drinking water by removing the dissolved salts from brackish or seawater to overcome the problem of water shortage. RO membrane has an asymmetric structure and has an ability to reject the monovalent ions [1]. Thin-film composite and cellulose acetate (CA) are the two major polymeric materials used in the fabrication of RO membranes [2]. CA is a favored polymer for membrane fabrication due to its accessibility, easy to processing, resist the attack by chlorine and convenient to functionalize [3,4]. However, the CA membrane is affected by the high salinity and increasing the salt content leads to high osmotic pressure which requires a high applied pressure to produce a good performance [5]. The asymmetric structure affects the CA membrane to be susceptible to compact at high pressure. The compaction process generates when the dense layer merges with the porous sublayer

* Corresponding author.

[6]. These operating conditions demand a membrane with high mechanical properties to withstand the high pressure. The support layer can be enhanced the CA-RO membrane mechanical strength by decreasing the membrane shrinkage [7,8]. In addition, to enhance the hydrophilicity of CA membrane the grafting and crosslinking processes can be carried on the top surface of CA [9–14]. Different monomers such as methyldiethylene glycol methacrylate, glycidyl methacrylate-g-polyethyl and 2-acrylamido-2-methylpropane sulfonic acid have been used previously in the membrane grafting [9,15,16]. On the other hand, ethylene glycol dimethacrylate, N,N′-methylenebisacrylamide and N,N,N′,N′-tetramethylethylenediamine are used as crosslinkers onto membrane surface [17,18]. Worthley et al. [19] prepared and modified the CA-RO membrane via polymeric grafting of 2-hydroxyethyl methacrylate.

The objective of this work is to fabricate polyetheleneterephthalate (PET)/polybutyleneterephthalate (PBT) nonwoven polyester fabric support asymmetric CA-RO membranes by phase inversion technique with different CA thicknesses to resist the high-pressure salt rejection without deformation. In addition, the supported CA-RO membranes are grafted and crosslinked with *n*-isopropyl acrylamide (N-IPAAm) and N,N′-methylenebisacrylamide (MBAAm), respectively to enhance the hydrophilicity and decrease surface roughness with an improvement of the performance. The water flux and salt rejection of the supported CA-RO and the modified membranes are evaluated by a crossflow cell under variable applied pressure.

2. Experimental work

2.1. Materials

1,4-Dioxane was purchased from Sigma-Aldrich (Germany) with the purity of 99% and the glacial acetic acid (purity > 99.8%) was supplied by Panreac Quimica S.A (Barcelona, Spain) and BDH AnalaR (England), respectively. Methanol (purity > 99.5%) and acetone (purity > 99%) were purchased from Labsolve (Lisbon, Portugal). Ethanol was delivered from Carlo Erba, Spain. CA of molecular weight of 100,000 g/mol with 39.8 wt.% acetyl was obtained from Aldrich. Flat polyester nonwoven fabric with a thickness of 120 μm (85 g/m²) based on PET/PBT of mechanical strength (200 N/5 cm), (Novatexx 2484) was purchased from Freudenberg Filtration Technologies Company, Germany. *N*-isopropyl acrylamide and N,N-methylene bisacrylamide were obtained from Across (New Jersey, USA). Potassium persulfate and NaOH were purchased from Sigma-Aldrich (Germany) and Carlo Erba, Spain, respectively. NaCl was supplied by Honeywell, Denmark.

2.2. Preparation of CA-RO membranes on nonwoven polyester

The solution mixture of acetone (13.5 ml), dioxane (27 ml), glacial acetic acid (5 ml) and methanol (10.7 ml) and CA (8.45 g) was cast on nonwoven fabric polyester as a support layer with different thicknesses of 100, 150, 200 and 250 μm using an automatic film applicator (Zehntner, Swiss) [9]. The phase inversion technique was applied to prepare the supported CA-RO membrane. Nonwoven fabric polyester was wetted with the glacial acetic acid for 30 min before casting the CA membrane. The evaporation time was 60 s and then the glass plate was immersed into ice-cold water at 4°C for 15 min to exchange the solvent with nonsolvent and this is followed by the precipitation process. The separated RO membrane from the glass plate was placed in another cold water bath at 4°C for 2 h. Finally, the thermal annealing of the RO-membrane was carried out by increasing the temperature gradually to 80°C for 10 min.

2.3. Grafting and crosslinking of supported CA-RO membranes

The mentioned above membrane supported with a thickness of 250 μm was grafted by 0.1% of N-IPAAm. Potassium persulfate with 1.5 wt.% was used as an initiator to form a free radical onto the surface of the CA active layer by the abstraction of a hydrogen atom from CA. Then the grafting process was carried out by spreading N-IPAAm solution on this active surface CA membrane and keeping for 10 min at room temperature [20]. The produced supported grafted CA-RO membrane was dried in an oven for 10 min at 40°C. Finally, the reaction of MBAAm as a crosslinker (0.013% of MBAAm to 0.1% N-IPAAm in 5% ethanol) on the surface of the supported grafted CA-RO membrane was accomplished.

2.4. Characterization techniques

Scanning electron microscopy (SEM), XL 5300 JEOL (Japan) has been used to study the morphology of the pure, grafted and crosslinked CA-RO membranes. The cross-sections of the RO membranes were imaged after cutting off under liquid N_2 for a consistent and clear break cross-section imaging and have been coated by a gold thin film using a sputter coating technique. Atomic force microscope (AFM) images of RO membranes were taken for three areas with 0.5 μm × 0.5 μm, 1 μm × 1 μm, and 5 μm × 5 μm using SPM-9700, Shimadzu (Japan) equipped with the dynamic mode at ambient temperature. A microcantilever OMCL-TR800PSA (Olympus) was used. The contact angles measurement was performed to evaluate the surface hydrophilicity by using a Ramé-Hart, Instrument Company, France and by fixing the membrane sample (3 cm × 2 cm) onto a glass plate by a double face tape. A droplet of 2 μL deionized water (2 μL) was placed on the active membrane surface using microsyringe (Hamilton Company, Reno, NV). The contact angles were measured on the right and left sides of the droplet. The average of six measurements was calculated.

2.5. Salt rejection and water flux measurements

The salt rejection and water flux of the prepared RO membranes were tested across flow stainless steel cells (CF042 Sterling Company) under different operating pressures. The hydraulic pump was used to apply the operating pressure and adjusted by a pressure gauge and follow by a pressure control valve with a variable frequency drive (SV015IG5A-4) and flow meter (F-550, USA). The membrane was first tested under constant pressure with deionized water for 30 min to open the channels and pores of the RO membrane. The feed solution was prepared by NaCl of 10,000 ppm and pH 7 at 25°C. The total dissolved

salts were measured by pH/conductivity meter 430 portable Jenway, UK.

The salt rejection (*R*) of the prepared membranes and calculated by the following equation [21]:

$$R = \left(1 - \frac{C_p}{C_f}\right) \times 100\% \qquad (1)$$

where C_p is the concentration of solute in permeate and C_f is the concentration of the solute in the feed.

The permeate water flux (*F*) represents the amount of the pure water per unit area per unit time at different pressures and is determined by Eq. (2) [21].

$$F = \frac{V}{t \times A} \qquad (2)$$

where *V* is the permeate volume, *A* is an area of active membrane and *t* is time.

3. Results and discussion

3.1. Mechanism of grafted/crosslinked supported CA-RO membrane

Supported CA-RO membrane is grafted by N-IPAAm via free radical polymerization using KPS as an initiator on the surface of the membrane. Firstly, the free radical formed by hydrogen abstraction of the cellulose hydroxyl group on the membrane surface and then N-IPAAm is reacted by the creating free radical on the terminal vinyl group which terminated by the crosslinker MBAAm as illustrated in Fig. 1.

3.2. Structural property of CA, grafted/CA and grafted/crosslinked RO membranes

Fig. 2 shows the Fourier-transform infrared spectroscopy of the supported CA, grafted and grafted/crosslinked CA-RO membranes. The spectra present characteristic broadband at 3,520 cm⁻¹ for OH stretching which becomes sharper at 3,500 and 3,510 cm⁻¹ for the grafted and grafted/crosslinked membranes due to the overlapping between the OH and N–H stretching of the amide groups of N-IPAAm and MBAAm. The absorption peaks at 2,947; 2,991 and 2,972 cm⁻¹ are attributed to the CH groups of pure, grafted and crosslinked membranes, respectively. The sharp absorption band at 1,743 cm⁻¹ corresponds to the carbonyl of the acetyl group of all the membranes. The appearance of the absorption bands at 1,668 and 1,676 cm⁻¹ are observed for the carbonyl in the amide group of N-IPAAm and MBAAm, respectively. In addition, the disappearance of the band at 1,640 cm⁻¹ confirms the grafting and crosslinking process of N-IPAAm and MBAAm on the vinyl group C=C. Moreover,
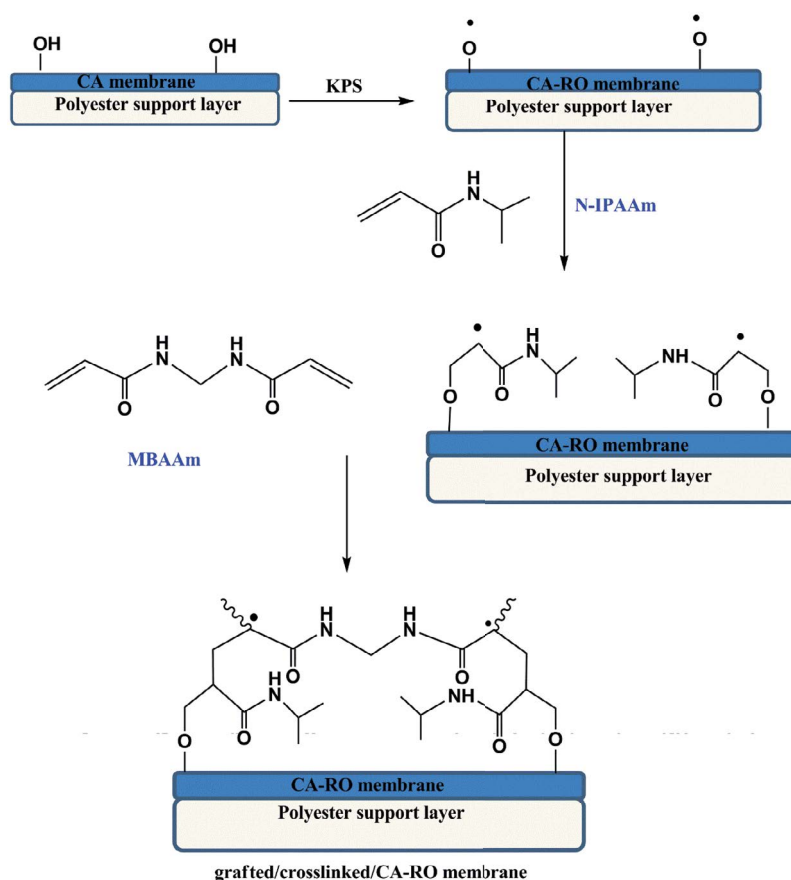

Fig. 1. Mechanism of grafting and crosslinking of supported CA-RO membrane with N-IPAAm and MBAAm.
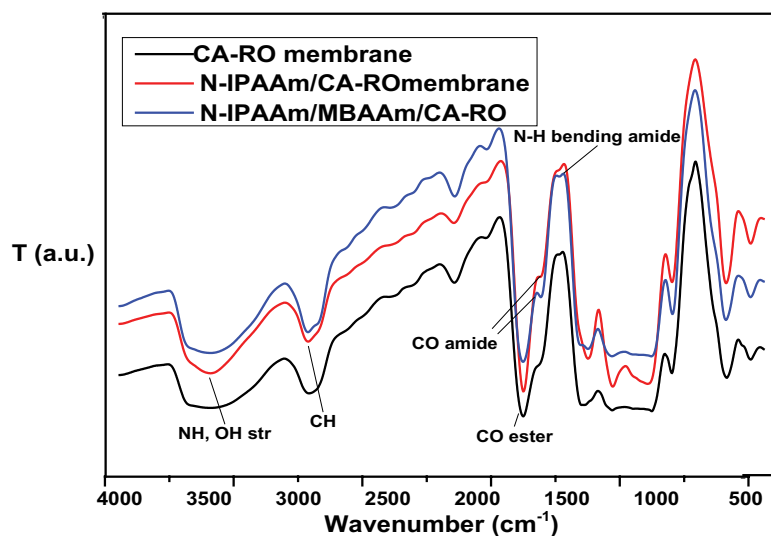
Fig. 2. Fourier-transform infrared spectroscopy of pristine supported CA/RO supported N-IPAAm/CA-RO and N-IPAAM/MBAAm/CA-RO membranes.

the weak absorption band at 1,545 cm^{-1} is assigned for the N–H bending in the MBAAm of the grafted/crosslinked CA-RO membrane [17,22].

3.3. Morphological studies

3.3.1. SEM analysis

Fig. 3 shows the morphology of top surface, bottom and cross-section of the different thicknesses 100, 150, 200 and 250 μm of CA-RO membranes cast onto nonwoven polyester fabric. The top surface of the lower thickness of 100 μm of CA displays a visible backing layer of fabric. There is an agglomeration of CA on the bottom due to the little impregnation of CA through the fabric nonwoven layer. The cross-section indicates the only one layer of the polyester without appearing of the dense layer of CA as shown in Fig. 3a.

The higher thicknesses of 150 and 200 μm CA improve the top surface morphology and covered the fabric layer. The wavy of polyester is decreased. However, the bottom surface forms two compatible and incompatible regions. The incompatible region is formed due to the low wetting of the backing layer with acetic acid before casting the polymer solution and penetration of CA through the nonwoven fabric layer as depicted in Figs. 3b and c. On the other hand, the compatible region results in a homogeneous phase of CA and polyester fabric.

The high thickness of 250 μm CA exhibits a smooth and fully covered top surface of the CA membrane. Therefore, the incompatible region at the bottom of the membrane is reduced. At this thickness, the cross-section illustrates and confirms the formation of an asymmetric CA membrane with a dense top layer and porous sublayer contains a macrovoid structure coated onto a support nonwoven polyester fabric as presented in Fig. 3d.

SEM images of the surface, bottom and cross-section of the pure supported CA-RO membrane, grafted supported CA and grafted/crosslinked supported CA-RO membranes

with 250 μm of CA are depicted in Fig. 4. The grafted CA membrane with N-IPAAm monomer exhibits a smoother top surface than the pure supported CA-RO membrane. The grafted CA membrane with N-IPAAm also enhances the formation of the three layers of the asymmetric RO membrane and a small finger-like macrovoid structure is formed as shown in the cross-section. However, the addition of the crosslinker MBAAm to the CA-RO membrane shows a formation of large numbers from a finger-like macrovoids structure with a homogenous distribution. Viscous fingering in presence of monomers or crosslinkers appears due to the instabilities at the interface to initiate the formation of finger-like voids. The relative thickness of finger-like and sponge-like regions greatly affects the properties of the membrane such as permeation water flux [23]. Increasing the number of macrovoids and finger-like structures confirms that the N-IPAAm and MBAAm may be acted as a pore former.

The morphology of the grafting and grafting/crosslinking process of CA cast on nonwoven polyester fabric is schematically presented in Fig. 5.

3.3.2. AFM analysis

AFM images analyze the membrane surface topology and determine the surface roughness. Fig. 6 shows the three dimensions views of AFM analysis of the pure supported CA/RO membrane, the grafted supported CA/RO membrane by 0.1% N-IPAAm and the crosslinked/grafted CA-RO membranes by 0.013% MBAAm. The bright regions represent the peaks and the dark regions are the valleys while the pores are mainly founded in the dark points. [24]. Characterization of the surfaces was achieved by measuring the roughness, average roughness, mean height, and peak-valley. Roughness is one of the most important surface properties as it has a strong influence on adhesion (fouling) and also on local mass transfer. The adhesive force has been shown to be larger for membranes with high
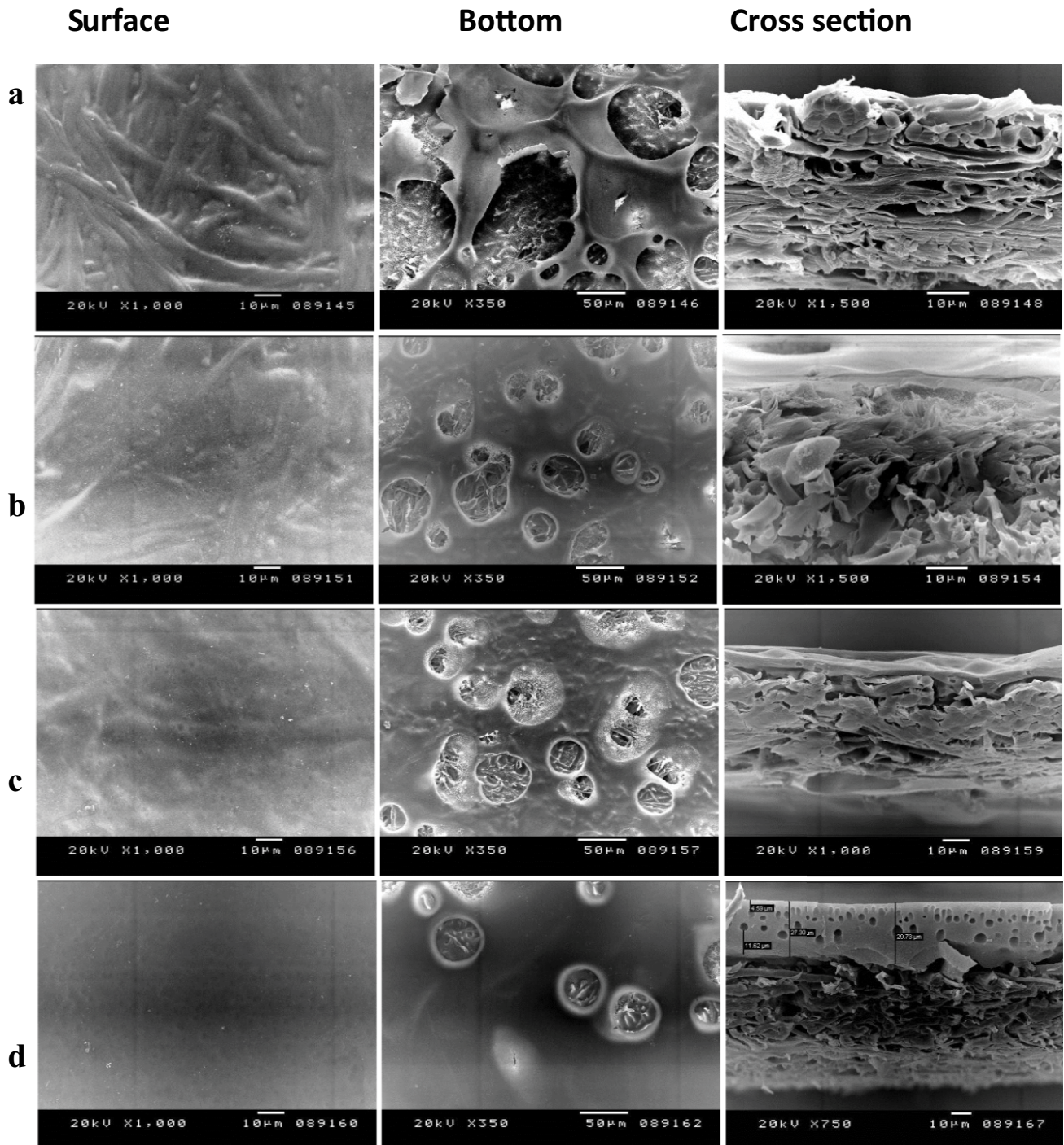
Surface	Bottom	Cross section

Fig. 3. SEM images of the surface, bottom and cross-section of CA-RO membranes cast on nonwoven fabric polyester (a) 100 μm, (b) 150 μm, (c) 200 μm, and (d) 250 μm supported CA-RO membrane.

roughness compared to the smooth membranes. A large number of peaks and valleys on the membrane surface affect the roughness average (R_a), difference average of the five height peaks and the lowest five valleys (R_z) and the root mean square (R_q) which calculated from AFM images [25]. Table 1 lists the parameters of three areas (0.5 μm² × 0.5 μm², 1 μm² × 1 μm² and 5 μm² × 5 μm²) of the pure and modified membranes. It is observed that R_a value of the membrane

area of 1 μm² × 1 μm² is 5.51 nm for the pure CA-RO, while R_a of the grafted and crosslinked CA-RO membranes are sharply decreased to 1.27 and 2.31 nm, respectively. In addition, R_z results in 44.4 nm for the purely supported membrane and decreases to 16.25 and 27.09 nm for the grafted and crosslinked membranes, respectively. Moreover, it is found that R_q is 7.06 nm for the pure CA-RO and declines to 1.66 and 3.04 nm for the modified grafted and crosslinked

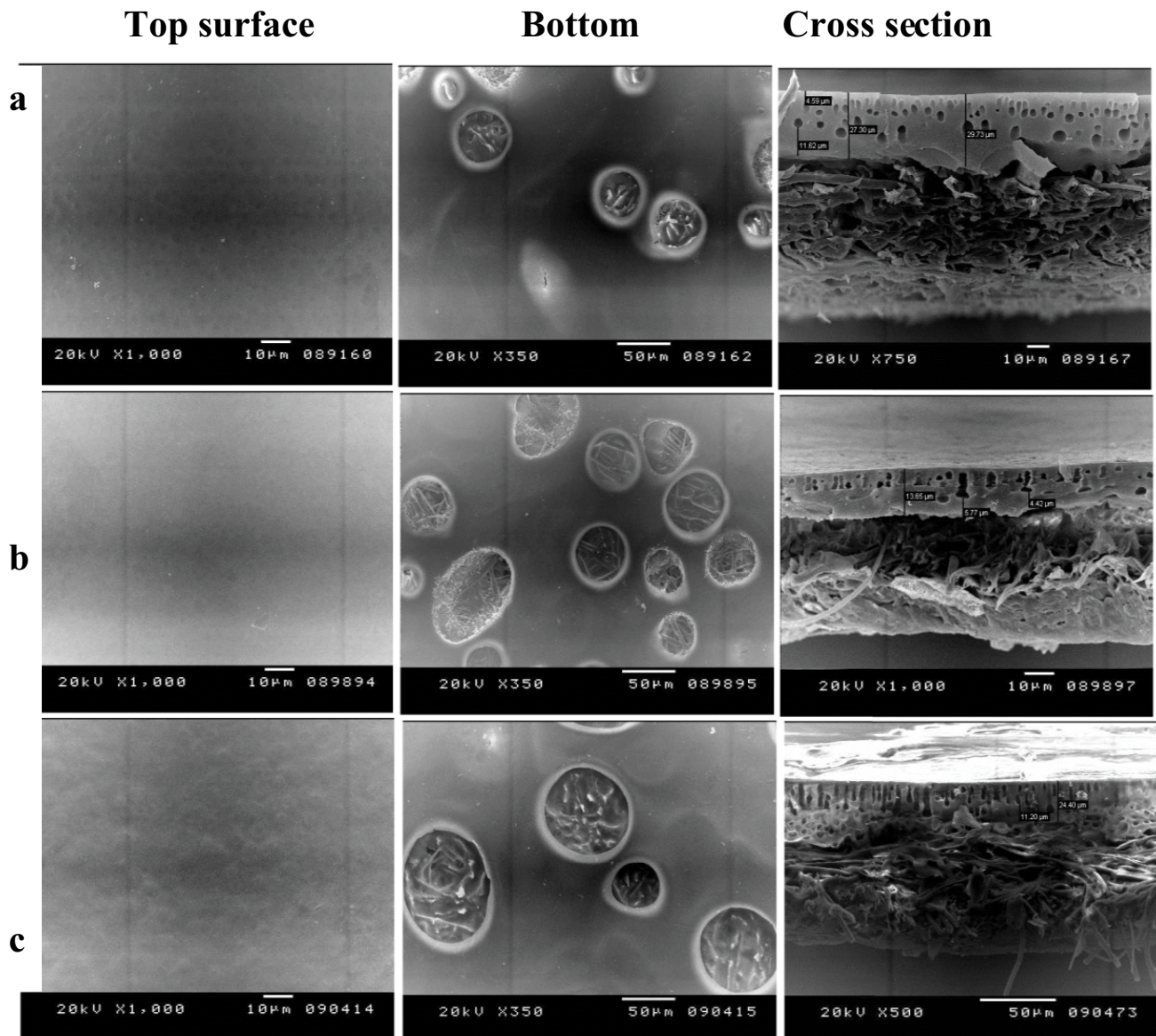**Top surface**   **Bottom**   **Cross section**

Fig. 4. SEM images of the surface, bottom and cross-section of (a) pure supported CA-RO membrane, (b) grafted CA-RO membrane and (c) crosslinked/grafted supported CA-RO membrane.

CA-RO membranes, respectively. It is clear that the CA-RO membrane has the highest value of roughness among the investigated membranes. This means that this membrane is expected to have a relatively high adhesive force and as the result high fouling on its surface. On the other hand, the crosslinked membrane has a low value of roughness while the grafting membrane has the lowest value of roughness [26]. From these data, we concluded that R_a, R_z and R_q values are significantly decreased with the grafting process due to the formation of homogeneous and dense top layers which decreases the wavy structure and treats the defects on the membrane surface [27]. However, the surface roughness of the crosslinked membrane is slightly increased than the grafted membrane due to the lower crosslinker solubility and the enhancing of the formation of the free volume between polymer chains of CA [28].

3.4. Effect of grafting and crosslinking on the surface hydrophilicity

The contact angle is used to evaluate the hydrophilicity of the membrane surface. The contact angles values of the active layer of different thicknesses of 100, 150, 200 and 250 μm of CA-RO membranes on nonwoven polyester are 59.86°, 59.82°, 59.02° and 59°, respectively as presented in Fig. 7a. This insignificant change in the values of contact angles is attributed to the fixed chemical structure and composition of the top surface. It is noted that CA membrane nature is a hydrophilic material due to the presence of the hydroxyl group in the CA chains [29,30].

Fig. 7b indicates the bar chart of the contact angles of CA, grafted CA and grafted/crosslinked CA-RO membranes. It is cleared that there is a sharp decrease in the
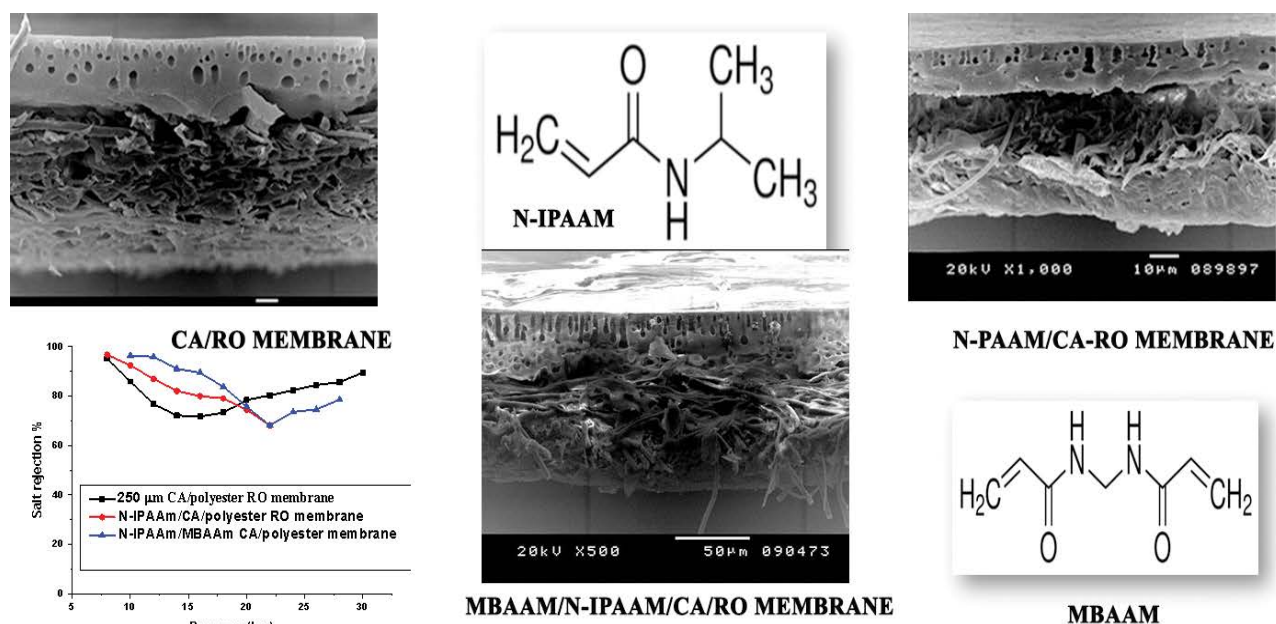
Fig. 5. Scheme of the grafting/crosslinking supported CA-RO membranes.

Table 1
AFM parameters of supported CA, 0.1 N-IPAAm grafted and 0.1 N-IPAAm grafted/0.013 MBAAm crosslinked RO membranes calculated by AFM (area 0.5 μm × 0.5 μm, 1 μm × 1 μm and 5 μm × 5 μm)

AFM parameters	R_a (nm)			R_z (nm)			R_q (nm)		
RO membranes	0.5 μm² × 0.5 μm²	1 μm² × 1 μm²	5 μm² × 5 μm²	0.5 μm² × 0.5 μm²	1 μm × 1 μm	5 μm² × 5 μm²	0.5 μm² × 0.5 μm²	1 μm² × 1 μm²	5 μm² × 1
Supported CA	3.05	5.51	13.71	26	44.4	164.9	3.93	7.06	18.8
Grafted/supported/CA	0.65	1.27	6.04	13.58	16.25	87.2	0.987	1.66	8.31
Crosslinked/grafted/ supported CA	1.17	2.31	8.47	10.06	27.09	122.6	1.46	3.04	11.7

contact angle from 59° to 44.38° for CA and the grafted CA membranes, respectively due to the hydrophilic properties of N-IPAAm contains C=O and N–H groups. Moreover, the addition of the crosslinker of the MBAAm decreases the contact angle of the CA membrane to 47.94° and this value is slightly higher than the grafted CA membrane. The cross-linker has the ability to links the polymer chains and providing a long chain of the polymer [27]. These results are in agreement with that obtained by Worthley et al. [19] where they found that the pristine CA membrane displayed an average contact angle of 70° ± 2° whereas pHEMA coated membranes (30 min) had an average contact angle of 75° ± 1°. CA-g-pHEMA60 had an average contact angle of 52° ± 2° [19].

3.5. Salt rejection and water flux of supported CA-RO membranes

3.5.1. Effect of CA-RO membrane thicknesses

The salt rejection and water flux of the supported CA-RO membranes cast with different thicknesses of 100, 150, 200 and 250 μm vs. the operating pressure are presented in Fig. 8. It is observed that the supported CA-RO

membrane with a thickness of 100 μm passes the water without separation of salts at low pressure. The thickness of the CA coating layer on the fabric support layer is not sufficient for the desalination process under the operating pressure. The salt rejections of CA-RO membranes with thicknesses of 150, 200 and 250 μm tested under operating pressure of 8 bar are 61.42%, 97.9% and 95.13%, respectively. When the operating pressure has increased to 16 bar, the salt rejections of the polyester/CA-RO membranes with thicknesses of 150, 200 and 250 μm decline to 25.9%, 76.34% and 71.84%, respectively. This can be explained based on the solute accumulation at the membrane surface that leads to the formation of a boundary layer of salt across the membrane and consequently this declines the driving force.

As illustrated in Eq. (3), the solute concentration C_m at the membrane surface increases, the permeate concentration C_p will increase and result in the salt rejection decreases [31].

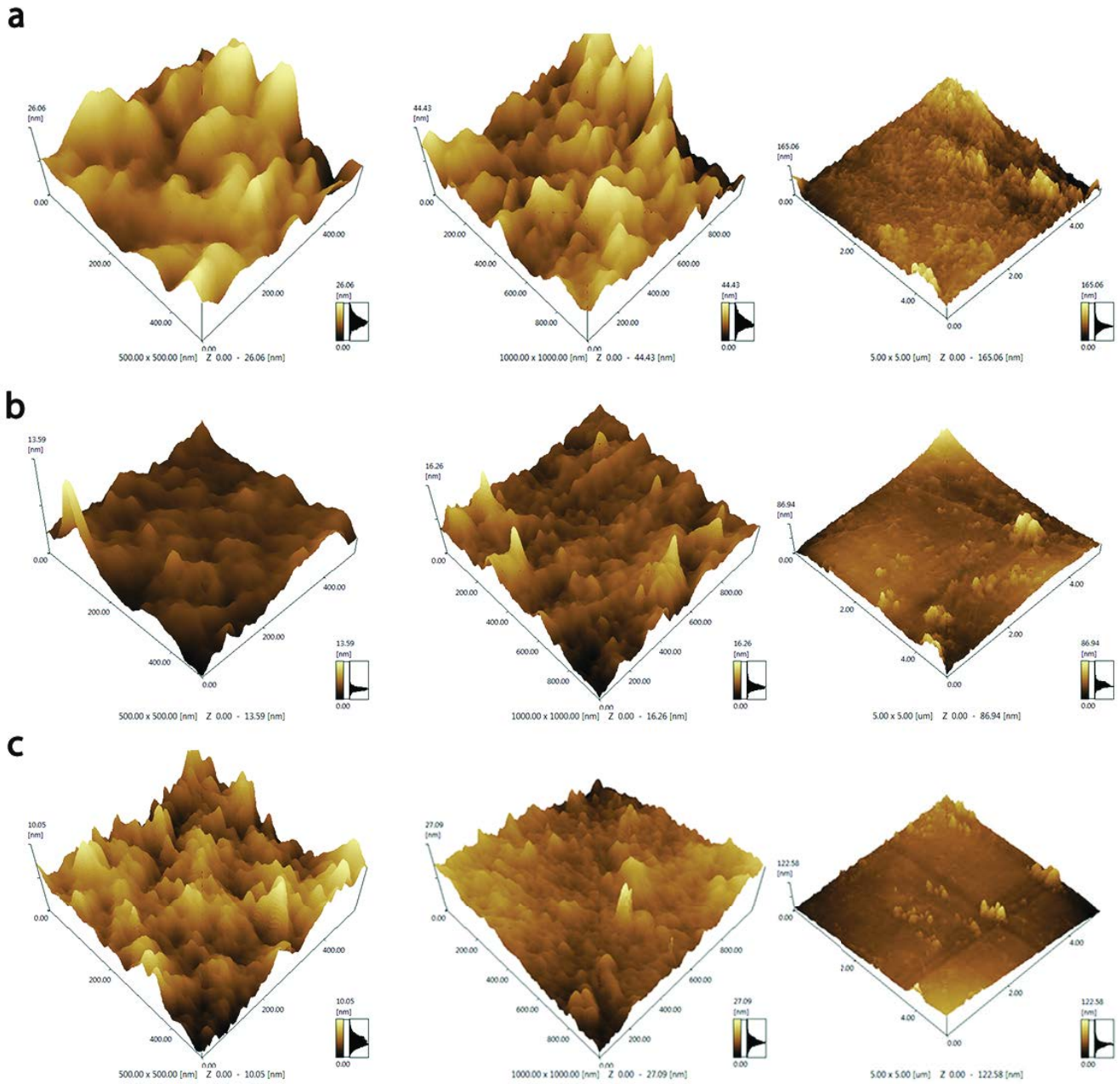$$R_r = 1 - \frac{C_p}{C_m} \qquad (3)$$

Fig. 6. AFM images of three dimensions areas of 0.5 μm × 0.5 μm, 1 μm × 1 μm and 5 μm × 5 μm of (a) supported CA-RO membrane, (b) grafted/supported CA-RO membrane and (c) crosslinked/grafted/supported CA-RO membrane.

Further increase in the operating pressure to 22 bar for the membrane with 150 μm thickness, the salt rejection is increased again to 49.55%. The salt rejections of the 200 and 250 μm thicknesses are raised to 81.2% and 80.3%, respectively at 22 bar as illustrated in Fig. 8a.

The salt rejection was increased again due to the effect of concentration polarization which starts to decrease during the separation process and consequently the diffusion of solute will reverse forward to the feed solution owing to the difference in the concentration of salts between membrane surface and the feed bulk. Increasing the net driving force results in a drop in the osmotic pressure, as indicated in Eq. (4) [31].

$$\Delta p_{\text{eff}} = \Delta p - \Delta \pi \tag{4}$$

where $\Delta \pi$ the osmotic pressure difference of the solution is across the membrane, Δp is the applied pressure and Δp_{eff} effective pressure or driving force.

Fig. 8b illustrates the water flux values of the above three supported CA-RO membranes. At low pressure of
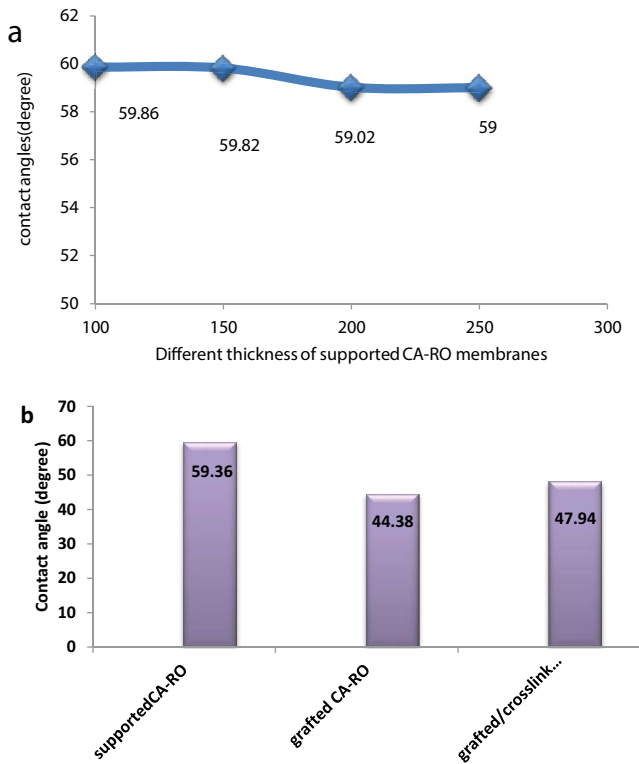
Fig. 7. Contact angles vs. thicknesses of supported CA-RO membrane (a), and contact angles of different types of RO membranes (b).

8 bar, water flux is 5.81 L/m²h which further increased to 14 L/m²h at 22 bar for 150 μm CA-RO. Furthermore, the higher thicknesses of 200 and 250 μm CA-RO membranes, the water flux values are started at 8 bar and exhibit initial results of 1.785 and 2.38 L/m²h, respectively. These values are increased gradually to 14.2 and 12.9 L/m²h by increasing the operating pressure to 22 bar. This is attributed to the increase of the transmembrane pressure forces through the membrane. Besides, it is found that the water flux is directly proportional to the applied pressure according to the following equation [32]:

$$F = A(\Delta p - \Delta \pi) \tag{5}$$

where A is the membrane constant. As the Δp increases, the $\Delta \pi$ decreases and the water flux will be higher.

3.5.2. Effect of grafted/crosslinked supported CA-RO membranes

Fig. 9 shows the influence of the grafting and crosslinking of the supported CA-RO membranes with a thickness of 250 μm on the salt rejections and water fluxes. The salt rejection values of pure supported CA, 0.1% N-IPAAm grafted supported CA and 0.1 N-IPAAm/0.013% MBAAm/supported CA-RO membranes are 85.91%, 92.4% and 96.4%, respectively at 10 bar. Increasing the applied pressure to 14 bar, the salt rejection results respectively, are obviously
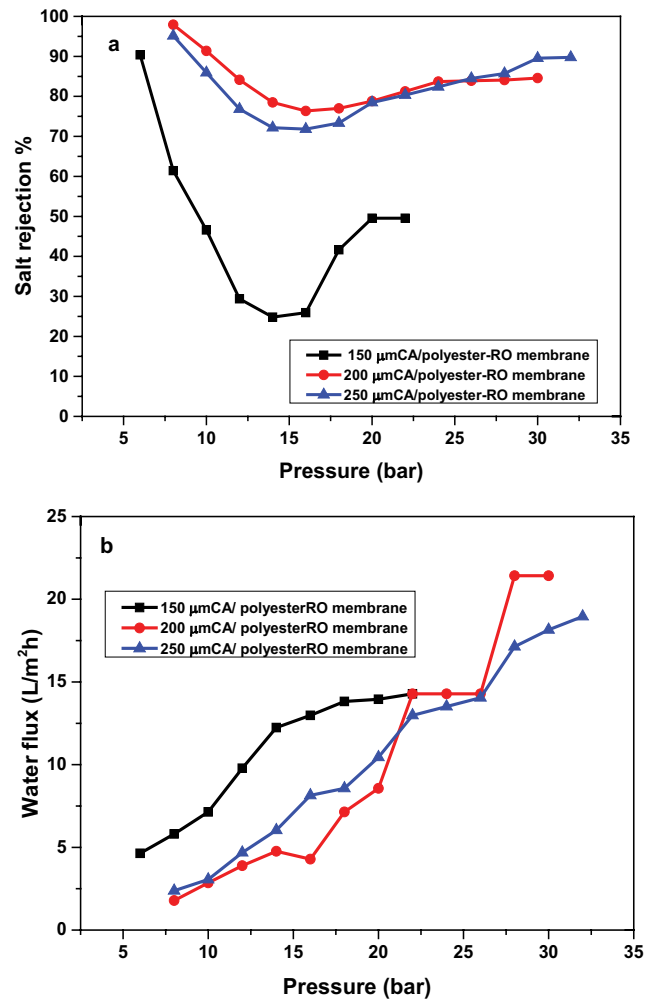

Fig. 8. (a) Salt rejection and (b) water flux of different thicknesses of CA cast on polyester RO membranes.

decreased to 72.15%, 82.11% and 91%. It is noted that the grafted and crosslinked CA-RO membrane exhibits higher stability on the rejection by raising the operating pressure. Furthermore, increasing the operating pressure to 28 bar, the salt rejections of the pure supported and grafted crosslinked/CA-RO membrane increased again to 89.76% and 78.6%, respectively as previously mentioned as shown in Fig. 9a. It is observed that the salt rejection of the grafted and crosslinked grafted membranes are higher than the pure supported CA-RO membranes. This is attributed to the formation of a homogeneous and compact layer of grafting on the surface and the formation of the network structure of N-IPAAm and the crosslinker MBAAm which could link the monomer free radicals and creating crosslinking between the polymer chain to increase the surface net structure [28]. When the N-IPAAm grafted membrane is crosslinked with MBAAm, the monomer's contents are increased and result in a higher salt rejection than the grafted membrane. It can be concluded that the crosslinked/supported CA-RO membrane with N-IPAAm/MBAAm displays an enhancement of the stability and separation performance.
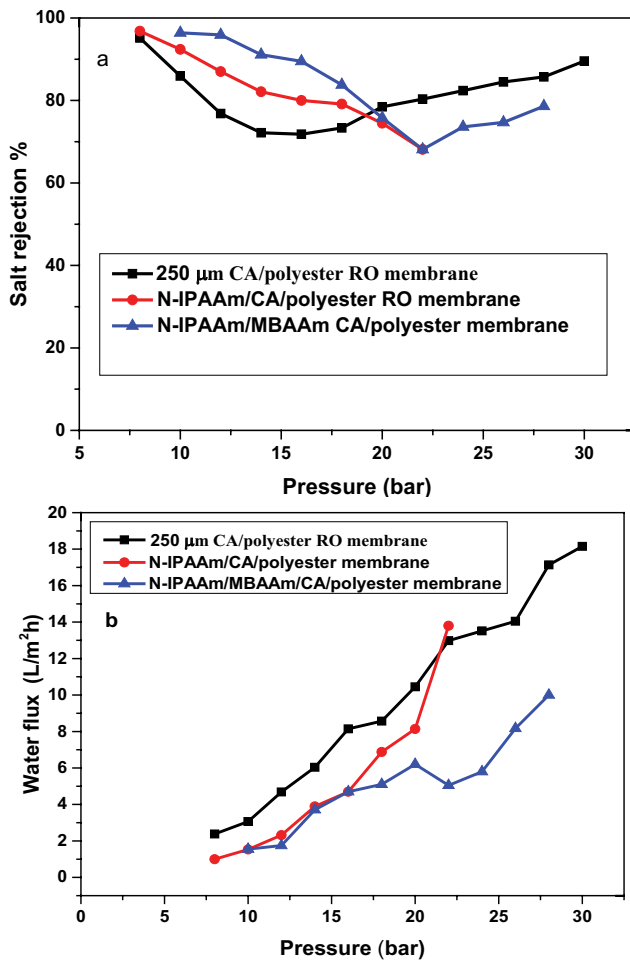
Fig. 9. (a) Salt rejection and (b) water flux of supported CA-RO membrane, grafted supported CA-RO membrane and grafted crosslinked CA-RO membrane.

Worthley et al. [19] found that the salt rejection of the pristine CA-RO membrane was 87.9% and decreased after grafting with pHEMA for 30 and 60 min to 83.1% and 20.4%, respectively.

The water fluxes at a low operating pressure of 10 bar are 3.06, 1.53 and 1.55 l/m²h for the pure supported, grafted supported and crosslinked/grafted supported CA-RO membranes, respectively. The operating pressure is increased to 14 bar and water flux values are increased to 6 L/m²h for the unmodified supported membrane, 3.89 L/m²h for the grafted membrane and 3.75 L/m²h for the crosslinked/grafted supported CA-RO membrane. When the pressure is further increased to 28 bar, the water flux of the grafted/crosslinked membranes is promoted to 10 L/m²h as shown in Fig. 9b. The higher water flux of the pure supported CA-RO membrane than the grafted and crosslinked is assigned to the penetration of the monomer through the membrane to the backing and blocking both of the pores and channels of the membrane. The grafting on the membrane surface could also increase the hydraulic resistance or the concentration polarization [33]. The layers of the grafted and crosslinked membranes cast on the fabric support layer increase the

compaction, where the grafting and crosslinking on the surface could rearrange the polymer chains and causing a lower water flux than the pure supported CA-RO membrane [34].

4. Conclusions

The asymmetric CA-RO membranes were prepared by casting different thicknesses of CA onto nonwoven polyester fabric as support to resist the high pressure and avoid the shrinkage of the membrane. The morphology of pure supported CA-RO membrane showed a macrovoids structure, while the grafted and crosslinked CA membranes displayed a fingerlike macrovoid structure. AFM image with an area of 1 μm × 1 μm exhibited R_a value of 5.51 nm for the pure supported CA-RO membrane which decreased to 1.27 nm and 2.31 nm for the grafted and grafted/crosslinked RO membranes, respectively. The hydrophilicity was increased with the grafted N-IPAAm/CA and crosslinked MBAAm/N-IPAAm CA-RO membranes than the pure membrane. The performance of the supported CA-RO membranes presented highly stable membranes under high operating pressure of 30 bar. The salt rejection values of pure supported CA, 0.1% N-IPAAm grafted supported CA and 0.1 N-IPAAm/0.013% MBAAm/supported CA-RO membranes were 85.91%, 92.4% and 96.4% at 10 bar. It was found that the water flux values were 6 L/m²h for the unmodified supported membrane, 3.89 L/m²h for the grafted membrane and 3.75 L/m²h for the crosslinked/grafted supported CA-RO membrane.

References

[1] G.M. Geise, H.-S. Lee, D.J. Miller, B.D. Freeman, J.E. McGrath, D.R. Paul, Water purification by membranes: the role of polymer science, J. Polym. Sci., Part B: Polym. Phys., 48 (2010) 1685–1718.

[2] K.P. Lee, T.C. Arnot, D. Mattia, A review of reverse osmosis membrane materials for desalination—development to date and future potential, J. Membr. Sci., 370 (2011) 1–22.

[3] H. Etemadi, R. Yegani, M. Seyfollahi, The effect of amino functionalized and polyethylene glycol grafted nanodiamond on anti-biofouling properties of cellulose acetate membrane in membrane bioreactor systems, Sep. Purif. Technol., 177 (2017) 350–362.

[4] X.-S. Fan, Z.-T. Liu, Z.-W. Liu, J. Lu, Cellulose acetate membrane synthesis from biomass of ramie, J. Appl. Polym. Sci., 117 (2010) 588–595.

[5] N.M. Wade, Technical and economic evaluation of distillation and reverse osmosis desalination processes, Desalination, 93 (1993) 343–363.

[6] J.W. Lee, J.H. Jang, H.-R. Chae, S.H. Lee, C.-H. Lee, P.-K. Park, Y.-J. Won, I.-C. Kim, A facile route to enhance the water flux of a thin-film composite reverse osmosis membrane: incorporating thickness-controlled graphene oxide into a highly porous support layer, J. Mater. Chem. A, 3 (2015) 22053–22060.

[7] M. Said, S. Ebrahim, A. Gad, S. Kandil, Performance and stability of diaminotoluene-based polyamide composite reverse osmosis membranes incorporated with additives and cast on polyester fabric, Desal. Water Treat., 86 (2017) 115–123.

[8] M.R. Bilad, E. Guillen-Burrieza, M.O. Mavukkandy, F.A. Al Marzooqi, H.A. Arafat, Shrinkage, defect and membrane distillation performance of composite PVDF membranes, Desalination, 376 (2015) 62–72.

[9] A. Morsy, S. Ebrahim, E.-R. Kenawy, T. Abdel-Fattah, S. Kandil, Grafted cellulose acetate reverse osmosis membrane using 2-acrylamido-2-methylpropanesulfonic acid for water

desalination, Water Sci. Technol. Water Supply, 57 (2016) 1046–1056.

[10] A. Bhattacharya, B.N. Misra, Grafting: a versatile means to modify polymers: techniques, factors and applications, Prog. Polym. Sci., 29 (2004) 767–814.

[11] K. Kato, E. Uchida, E.-T. Kang, Y. Uyama, Y. Ikada, Polymer surface with graft chains, Prog. Polym. Sci., 28 (2003) 209–259.

[12] Y. Uyama, K. Kato, Y. Ikada, Surface Modification of Polymers by Grafting, In: Grafting/Characterization Techniques/Kinetic Modeling, Springer, Berlin, Heidelberg, 1998, pp. 1–39.

[13] B. Zhao, W.J. Brittain, Polymer brushes: surface-immobilized macromolecules, Prog. Polym. Sci., 25 (2000) 677–710.

[14] M. Amiji, K. Park, Surface modification of polymeric biomaterials with poly(ethylene oxide), albumin, and heparin for reduced thrombogenicity, J. Biomater. Sci., Polym. Ed., 4 (1993) 217–234.

[15] M. Billy, A.R. Da Costa, P. Lochon, R. Clément, M. Dresch, S. Etienne, J.M. Hiver, L. David, A. Jonquières, Cellulose acetate graft copolymers with nano-structured architectures: synthesis and characterization, Eur. Polym. J., 46 (2010) 944–957.

[16] A. Jayalakshmi, I.-C. Kim, Y.-N. Kwon, Cellulose acetate graft-(glycidylmethacrylate-*g*-PEG) for modification of AMC ultrafiltration membranes to mitigate organic fouling, RSC Adv., 5 (2015) 48290–48300.

[17] G.H. Zou, J. Shen, P.Z. Duan, X. Xia, R.G. Chen, B. Jin, Temperature-sensitive poly(*n*-isopropyl acrylamide)/konjac glucomannan/graphene oxide composite membranes with improved mechanical property, swelling capability, and degradability, J. Polym. Sci., 2018 (2018) 1–10, https://doi.org/10.1155/2018/7906747.

[18] A. Bhattacharya, P. Ray, Chapter 2 – Basic Features and Techniques, A. Bhattacharya, J.W. Rawlins, P. Ray, Eds., Polymer Grafting and Crosslinking, John Wiley & Sons, Inc., Hoboken, New Jersey, 2009, pp. 7–64.

[19] C.H. Worthley, K.T. Constantopoulos, M. Ginic-Markovic, R.J. Pillar, J.G. Matisons, S. Clarke, Surface modification of commercial cellulose acetate membranes using surface-initiated polymerization of 2-hydroxyethyl methacrylate to improve membrane surface biofouling resistance, Desalination, 273 (2011) 299–307.

[20] R. Kumar, R. Kr. Sharma, A.P. Singh, Grafting of cellulose with *N*-isopropyl acrylamide and glycidyl methacrylate for efficient removal of Ni(II), Cu(II) and Pd(II) ions from aqueous solution, Sep. Purif. Technol., 219 (2019) 249–259.

[21] M.S.F. Dasilva, Polyamide and Polyetherimide Organic Solvent Nanofiltration Membranes, Dissertation, University of Nova De Lisboa, 2007.

[22] C. Gorey, I.C. Escobar, *N*-isopropyl acrylamide (N-IPAAM) modified cellulose acetate ultrafiltration membranes, J. Membr. Sci., 383 (2011) 272–279.

[23] B.F. Kingsbury, K.A. Li, Morphological study of ceramic hollow fiber membranes, J. Membr. Sci., 328 (2009) 134–140.

[24] S. Waheed, A. Ahmad, S. Maqsood Khan, Sabad-e-Gul, T. Jamil, A. Islam, T. Hussain, Synthesis, characterization, permeation and antibacterial properties of cellulose acetate/polyethylene glycol membranes modified with chitosan, Desalination, 351 (2014) 59–69.

[25] M. Raposo, Q. Ferreira, P.A. Ribeiro, A Guide for Atomic Force Microscopy Analysis of Soft-Condensed Matter, A. Méndez-Vilas, J. Díaz, Eds., Modern Research and Educational Topics in Microscopy, FORMATEX, Badajoz, Spain, 2007.

[26] N. Hilal, H. Al-Zoubi, N.A. Darwish, A.W. Mohammad, Characterisation of nanofiltration membranes using atomic force microscopy, Desalination, 177 (2005) 187–199.

[27] Z. Zhang, Z. Wang, J.X. Wang, S.C. Wang, Enhancing chlorine resistances and anti-biofouling properties of commercial aromatic polyamide reverse osmosis membranes by grafting 3-allyl-5,5-dimethylhydantoin and N,N'-Methylenebis(acrylamide), Desalination, 309 (2013) 187–196

[28] H. Kamal, F.M. Abd-Elrahim, S. Lotfy, Characterization and some properties of cellulose acetate-co-polyethylene oxide blends prepared by the use of gamma irradiation, J. Radiat. Res. Appl. Sci., 7 (2014) 146–153.

[29] A. Halim, Y.C. Xu, K.-H. Lin, M. Kobayashi, M. Kajiyama, T. Enomae, Fabrication of cellulose nanofiber-deposited cellulose sponge as an oil-water separation membrane, Sep. Purif. Technol., 224 (2019) 322–331.

[30] J.R. McCutcheon, M. Elimelech, Influence of membrane support layer hydrophobicity on water flux in osmotically driven membrane processes, J. Membr. Sci., 318 (2008) 458–466.

[31] S. Bhattacharjee, Concentration Polarization: Early Theories, Water Planet, Inc., 8915 South La Cienega Avenue, Los Angeles, CA 90301 USA, 2017, pp. 1–10.

[32] M. Theresa, M. Pendergast, J.M. Nygaard, A.K. Ghosh, E.M.V. Hoek, Using nanocomposite materials technology to understand and control reverse osmosis membrane compaction, Desalination, 261 (2010) 255–263.

[33] R. Pang, K.S. Zhang, High-flux polyamide reverse osmosis membranes by surface grafting 4-(2-hydroxyethyl)morpholine, RSC Adv., 7 (2017) 40705–40710.

[34] E. Dimitriou, P. Boutikos, E. Sh. Mohamed, S. Koziel, G. Papadakis, Theoretical performance prediction of a reverse osmosis desalination membrane element under variable operating conditions, Desalination, 419 (2017) 70–78.